Hindawi
Journal of Applied Mathematics
Volume 2024, Article ID 2130429, 11 pages
https://doi.org/10.1155/2024/2130429

Research Article

The Significance of Stochastic CTMC Over Deterministic Model in Understanding the Dynamics of Lymphatic Filariasis With Asymptomatic Carriers

Mussa A. Stephano,[1,2] **Jacob I. Irunde**,[2] **Maranya M. Mayengo**,[1] **and Dmitry Kuznetsov**[1]

[1]*Department of Applied Mathematics and Computational Science, The Nelson Mandela African Institution of Science and Technology, P.O. Box 447, Arusha, Tanzania*
[2]*Department of Mathematics, Physics and Informatics, Mkwawa University College of Education, P.O. Box 2513, Iringa, Tanzania*

Correspondence should be addressed to Mussa A. Stephano; stephanom@nm-aist.ac.tz

Received 26 October 2023; Revised 9 April 2024; Accepted 17 April 2024; Published 4 May 2024

Academic Editor: Arvind Kumar Misra

Lymphatic filariasis is a leading cause of chronic and irreversible damage to human immunity. This paper presents deterministic and continuous-time Markov chain (CTMC) stochastic models regarding lymphatic filariasis dynamics. To account for randomness and uncertainties in dynamics, the CTMC model was formulated based on deterministic model possible events. A deterministic model's outputs suggest that disease extinction is feasible when the secondary threshold infection number is below one, while persistence becomes likely when the opposite holds true. Furthermore, the significant contribution of asymptomatic carriers was identified. Results indicate that persistence is more likely to occur when the infection results from asymptomatic, acutely infected, or infectious mosquitoes. Consequently, the CTMC stochastic model is essential in capturing variabilities, randomness, associated probabilities, and validity across different scales, whereas oversimplification and unpredictability of inherent may not be featured in a deterministic model.

Keywords: asymptomatic carriers; CTMC stochastic model; deterministic model; lymphatic filariasis; multitype branching process

1. Introduction

The nematode family of microfilarial parasites transmitted by mosquito-vector causing lymphatic filariasis commonly results in the chronic manifestation known as elephantiasis [1]. This disease is prevalent in tropical regions, especially in developing countries, where it often receives insufficient attention [2, 3]. Lymphatic system weakening, physical deformities, and long-term disability significantly impact the quality of life of affected individuals [4, 5].

Humans and mosquitoes serve as the definitive-primary and intermediate hosts of the parasites, respectively [4, 6]. In definitive-primary host, it presents three different stages, namely, asymptomatic carriers, acute, and chronic infected as illustrated in Figure 1. The asymptomatic stage exhibits nonvisible symptoms of infection, yet the parasites can still cause an impact on the immunity, facilitating the infection. In the acute stage, adenolymphangitis, a localized inflammation of lymph nodes and vessels, accompanied by skin problems is characterized. In the chronic stage, it progresses to hydrocele, lymphedema, compromised mental well-being, and elephantiasis [1, 4].

Lymphatic filariasis is a global health concern, exhibiting varying prevalence rates across different regions. It is transmitted by different mosquito vectors depending on the nematode species involved. The World Health Organization (WHO) in collaboration with governments recommended the implementation of mass drug administration (MDA) programs targeting both infected populations and those at risk [1]. Despite these efforts, the persistent prevalence of the disease emphasizes an urgent need for comprehensive research on its transmission dynamics to support

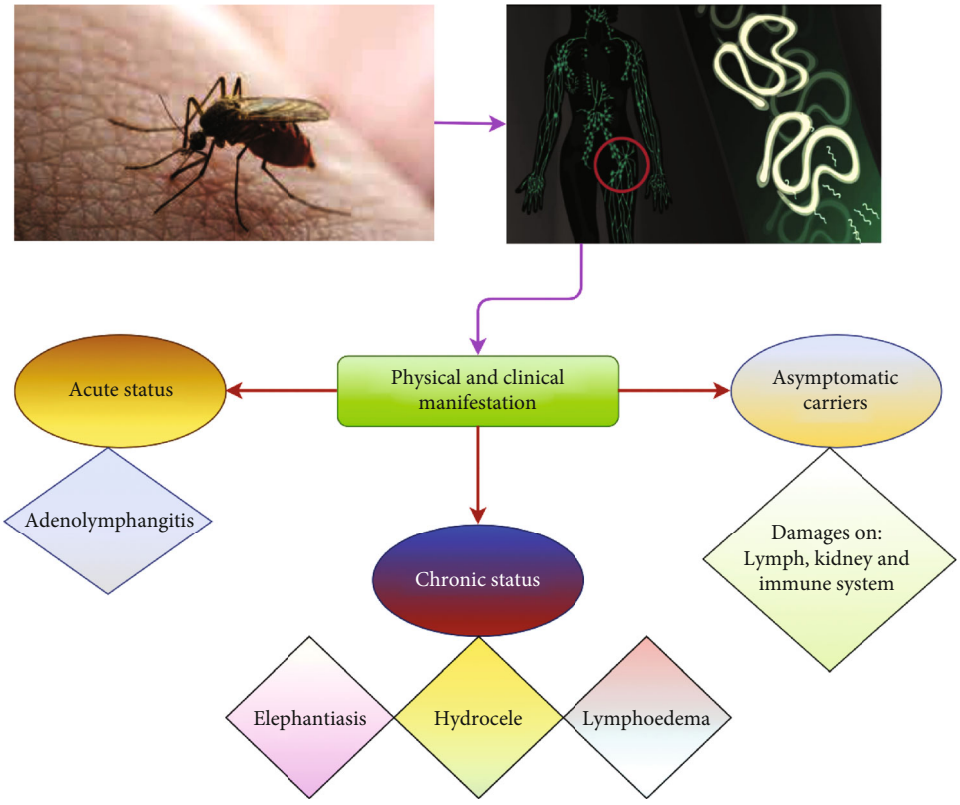

Figure 1: The life cycle of parasites, clinical manifestations, and physical condition [1, 4, 16, 17].

eradication initiatives, aligning with Sustainable Development Goal 3 and the roadmap for eliminating neglected tropical diseases by 2030.

Mathematical modelling has been used to address lymphatic filariasis in different aspects. The key and fundamental studies include Mwamtobe et al. [7], who introduced a model on humans and mosquitoes and concluded that treatment is more effective than quarantine. Jambulingam et al. [8] worked on a statistical model with a hypothesis on MDA with respect to the burden in India, highlighting that the MDA duration is proportional to the endemicity baseline. Michael et al. [9] addressed the MDA efficacy and control with albendazole and diethylcarbamazine in combination. Swaminathan et al. [10] worked on challenges with the aspect of prospects targeting the elimination of the disease, and Cromwell et al. [11] developed a geospatial distribution between 2000 and 2018.

Regarding the convolution of the life cycle of the microfilarial parasites in both two hosts, modelling the interaction and spread mode is of significant importance when including stochasticity. Nevertheless, the existing models did not incorporate stochastic behavior in dynamics. The significance of the CTMC model is that it captures variabilities and uncertainties that arise due to environmental variations and demographics and also predicts the probabilities of extinction or outbreak in finite time and studies the random sample path solutions near disease-free and endemic equilibria [12–15]. This paper presents a stochastic CTMC model based on the modified existing deterministic models of lymphatic filariasis dynamics.

2. Model Formulation

2.1. A Deterministic Model. The formulation of the model that depicts the dynamics of lymphatic filariasis in both definitive-primary and intermediate hosts is based on assumptions that the vertical transmission is not accounted for by the exclusion of immigration considerations, adherence to the mass action principle for the rate of infection [17], and the occurrence of induced mortality in the class of infected chronic only. Figure 2 visually represents the dynamic modification of the work by Jambulingam et al. [8], Mwamtobe et al. [7], Stolk et al. [18], and Swaminathan et al. [10].

The human population is divided into five groups: susceptible $S_1(t)$, exposed $E_1(t)$, asymptomatic $A(t)$, infected in the acute state $I_1(t)$, and infected in the chronic state $I_2(t)$. Similarly, the mosquito population comprises susceptible $S_2(t)$, exposed $E_2(t)$, and infected $I_3(t)$.

$S_1(t)$ recruited at a rate π_1, move to $E_1(t)$ being bitten by $I_3(t)$ at a rate β. A considerable number of individuals progress to $A(t)$ at a rate α, while the remaining proportion progress to either $I_1(t)$ at a rate ψ or I_2 at a rate ρ. Moreover, $A(t)$ progress to either $I_1(t)$ at a proportion of ξ or $I_2(t)$ at a rate ϕ. $I_1(t)$ progress to $I_2(t)$ at a rate σ. $I_2(t)$ induce death at a rate δ, and humans die naturally at a rate of μ_h.

π_2 is the recruitment rate of $S_2(t)$, exposed to lymphatic filariasis with either $A(t)$, $I_1(t)$, or $I_2(t)$ defined by general rate (Equation (1)):

$$\lambda = \beta_1 A + \beta_2 I_1 + \beta_3 I_2 \tag{1}$$

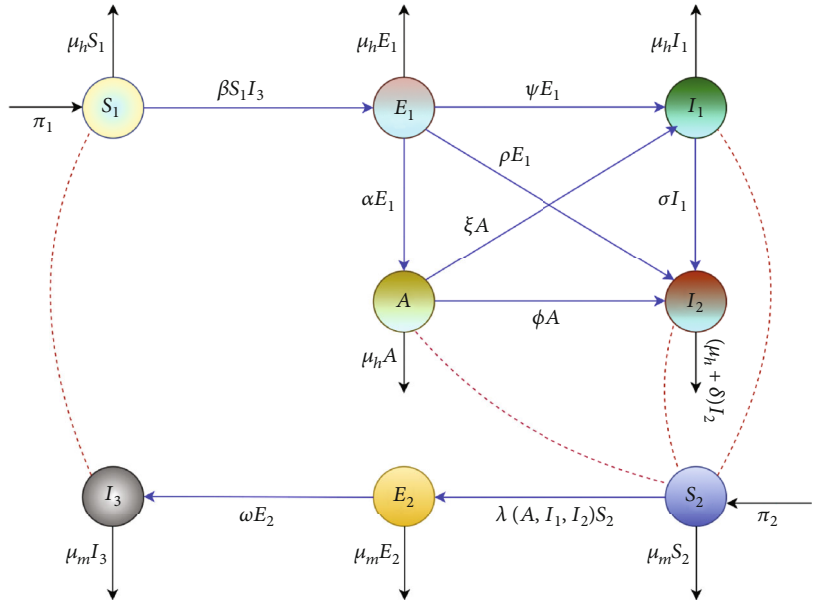

Figure 2: Compartments and CTMC possible events of interactions and transitions.

where β_1, β_2, and β_3 are transmission rates for S_2 from $A(t)$, $I_1(t)$, and I_2, respectively. $E_2(t)$ progress to $I_3(t)$ at a pace ω, and the natural mortality rate of mosquitoes is μ_m.

Model (2) represents the epidemiological interactions and transitions using a nonlinear system from Figure 2.

$$\begin{cases} \dfrac{dS_1(t)}{dt} = \pi_1 - \beta I_3 S_1 - \mu_h S_1 \\ \dfrac{dE_1(t)}{dt} = \beta I_3 S_1 - (\alpha + \rho + \psi + \mu_h) E_1 \\ \dfrac{dA(t)}{dt} = \alpha E_1 - (\xi + \phi + \mu_h) A \\ \dfrac{dI_1(t)}{dt} = \psi E_1 + \xi A - (\sigma + \mu_h) I_1 \\ \dfrac{dI_2(t)}{dt} = \rho E_1 + \phi A + \sigma I_1 - (\delta + \mu_h) I_2 \\ \dfrac{dS_2(t)}{dt} = \pi_2 - \lambda S_2 - \mu_m S_2 \\ \dfrac{dE_2(t)}{dt} = \lambda S_2 - (\omega + \mu_m) E_2 \\ \dfrac{dI_3(t)}{dt} = \omega E_2 - \mu_m I_3 \end{cases} \tag{2}$$

Bounded by

$S_2(0) > 0,\ E_1 0) \geq 0,\ A(0) \geq 0,\ I_1(0) \geq 0,\ I_2(0) \geq 0,\ S_1(0) > 0,\ E_2(0) \geq 0$, and $I_3(0) \geq 0$

2.2. Model Analysis. The dynamical system described by Equation (2) is subjected to evaluate its mathematical well-posedness and biological feasibility within the region $\{(S_1, E_1, A, I_1, I_2, S_2, E_2, I_3) \in \mathbb{R}_+^8\}$.

2.2.1. Positivity. To demonstrate the positivity of model solutions for all $t \geq 0$, let $\{t > 0 : S_1 > 0, E_1 > 0, A > 0, I_1 > 0, I_2 > 0, S_2 > 0, E_2 > 0, I_3 > 0\}$, $N_1 = S_1 + E_1 + A + I_1 + I_2$, and $N_2 = S_2 + E_2 + I_3$.

From the equation governing susceptible humans in Model (2),

$$\frac{dS_1(t)}{dt} = \pi_1 - \beta I_3 S_1 - \mu_h S_1$$

Assuming $S_1(0) > 0$ and $\exists t = t_0 > 0$, where $S_1(t_0) = 0$, $dS_1(t_0)/dt < 0$, $E_1(t_0) \geq 0$, $A(t_0) \geq 0$, $I_1(t_0) \geq 0$, $I_2(t_0) \geq 0$, $S_2(t_0) > 0$, $E_2(t_0) \geq 0$, and $I_3(t_0) \geq 0$, it follows:

$$\frac{dS_1(t_0)}{dt} = \pi_1 - \beta I_3(t_0) S_1(t_0) - \mu_h S_1(t_0) = \pi_1 > 0 \tag{3}$$

This contradicts the assumption, hence $S_1(t) > 0$ for all $t > 0$. Applying a similar method as used to get Equation (3), then Model (2) is positive invariant $\forall t > 0$.

2.2.2. Boundedness. By considering the total population of humans and mosquitoes separately, we have

$$\begin{cases} \dfrac{dN_1}{dt} \leq \pi_1 - \mu_h N_1 \\ \dfrac{dN_2}{dt} \leq \pi_2 - \mu_m N_2 \end{cases} \tag{4}$$

From Equation (4), the first population using integration techniques leads

$$N_1(t) \leq \frac{\pi_1}{\mu_h} + \left(N_1(0) - \frac{\pi_1}{\mu_h} \right) e^{-\mu_h t} \tag{5}$$

Applying the standard comparison theorem [19], when $N_1(0) > \pi_1/\mu_h$ and $N_1(0) < \pi_1/\mu_h$, we obtain

$$\begin{cases} \dfrac{\pi_1}{\mu_h} \le N_1(t) \le \dfrac{\pi_1}{\mu_h} + \left(N_1(0) - \dfrac{\pi_1}{\mu_h}\right)e^{-\mu_h t} \text{ and} \\ \dfrac{\pi_1}{\mu_h} + \left(N_1(0) - \dfrac{\pi_1}{\mu_h}\right)e^{-\mu_h t} \le N_1(t) \le \dfrac{\pi_1}{\mu_h} \end{cases} \tag{6}$$

With time approaching to infinity, it follows that

$$\begin{cases} 0 \le N_1(t) \le \dfrac{\pi_1}{\mu_h} \\ 0 \le N_2(t) \le \dfrac{\pi_2}{\mu_m} \end{cases} \tag{7}$$

Consequently, Model (2) is bounded within the region $\{(S_1, E_1, A, I_1, I_2, S_2, E_2, I_3) \in \mathbb{R}_+^8\}$.

2.3. Filariasis Free Equilibrium E_0 and Basic Reproduction Number $\mathscr{R}_0$

2.3.1. Filariasis Free Equilibrium. The context involves the extinction of parasites from populations, leading to a disease-free equilibrium denoted as E_0, which signifies the absence of lymphatic filariasis.

$$E_0 = \left(\frac{\pi_1}{\mu_h}, 0, 0, 0, 0, \frac{\pi_2}{\mu_m}, 0, 0\right) \tag{8}$$

2.3.2. Basic Reproduction Number $\mathscr{R}_0$. The computation of $\mathscr{R}_0$, with the help of the next-generation matrix technique evaluated at E_0, is given by

$$\mathscr{R}_0 = \frac{1}{\mu_m}\sqrt{\frac{\omega\beta\pi_1\pi_2}{\mu_h}\frac{(\mathscr{R}_{01} + \mathscr{R}_{02} + \mathscr{R}_{03} + \alpha\beta_2\eta_3)}{\eta_1\eta_2\eta_3\eta_4\eta_5}} \tag{9}$$

whereby

$$\begin{cases} \eta_1 = (\alpha + \rho + \psi + \mu_h), \eta_2 = (\xi + \phi + \mu_h) \\ \eta_3 = (\sigma + \mu_h), \eta_4 = (\delta + \mu_h), \eta_5 = (\omega + \mu_m) \\ \mathscr{R}_{01} = \beta_1\alpha(\xi\sigma + \phi\eta_3) \\ \mathscr{R}_{02} = \eta_2(\sigma\psi + \rho\eta_3) \\ \mathscr{R}_{03} = \eta_4(\beta_3\alpha\xi + \phi\eta_2) \end{cases}$$

where $\mathscr{R}_0$ represents the threshold value of infections after initial states generated by one infection in susceptible individuals throughout the period of infection [20].

2.3.3. Global Stability of E_0

Theorem 1. *The filariasis-free equilibrium E_0 is globally asymptotically stable when $\mathscr{R}_0 < 1$ and unstable otherwise.*

We decompose System (2) following the Metzler matrix technique as used in Stephano et al. and Castillo-Chavez and Song [17, 21]. Let $\boldsymbol{u}_1$ stands for (S_1, S_2), while $\boldsymbol{u}_2$ stands for $(E_1, A, I_1, I_2, E_2, I_3)$. Therefore, Model (2) can be decomposed to:

$$\begin{cases} \dfrac{d\boldsymbol{u}_1}{dt} = B_1(\boldsymbol{u}_1 - E_0) + B_2\boldsymbol{u}_2 \\ \dfrac{d\boldsymbol{u}_2}{dt} = B_3\boldsymbol{u}_2 \end{cases} \tag{10}$$

where

$$B_1 = \begin{pmatrix} -\mu_h & 0 \\ 0 & -\mu_m \end{pmatrix}, B_2 = \begin{pmatrix} 0 & 0 & 0 & 0 & 0 & -\dfrac{\beta\pi_1}{\mu_h} \\ 0 & \dfrac{\beta_2\pi_2}{\mu_m} & \dfrac{\beta_3\pi_2}{\mu_m} & \dfrac{\beta_1\pi_2}{\mu_m} & 0 & 0 \end{pmatrix}$$

$$B_3 = \begin{pmatrix} -(\alpha + \rho + \psi + \mu_h) & 0 & 0 & 0 & 0 & \dfrac{\beta\pi_1}{\mu_h} \\ \alpha & -(\xi + \phi + \mu_h) & 0 & 0 & 0 & 0 \\ \psi & \xi & -(\sigma + \mu_h) & 0 & 0 & 0 \\ \rho & \phi & \sigma & -(\delta + \mu_m) & 0 & 0 \\ 0 & \dfrac{\beta_2\pi_2}{\mu_m} & \dfrac{\beta_3\pi_2}{\mu_m} & \dfrac{\beta_1\pi_2}{\mu_m} & -(\omega + \mu_m) & 0 \\ 0 & 0 & 0 & 0 & \omega & -\mu_m \end{pmatrix}$$

Matrix B_1 has negative eigenvalues which determine that matrix B_3 is a Metzler matrix. Given that the nondiagonal components of matrix B_3 exhibit positivity, it is clear that E_0 is globally asymptotically stable.

2.4. Filariasis Endemic Equilibrium E^*. In the situation of persistence of lymphatic filariasis, the nontrivial point is computed from Model (2). It is denoted by $E^* = (S_1^*, E_1^*, A^*, I_1^*, I_2^*, S_2^*, E_2^*, I_3^*) \in \mathbb{R}_+^8$, such that

$$\begin{cases} S_1^* = \dfrac{\pi_1}{\beta I_3^* + \mu_h}, E_1^* = \dfrac{\beta\omega\mu_h\pi_1\pi_2(\mathscr{R}_0^2 - 1)}{\eta_1\mu_h(\beta\omega\pi_2 + \eta_5\mu_m\mu_h)\mathscr{R}_0^2} \\ A^* = \dfrac{\alpha\omega\mu_h\beta\pi_2\pi_1(\mathscr{R}_0^2 - 1)}{\eta_1\eta_2\mu_h(\beta\omega\pi_2 + \eta_5\mu_m\mu_h)\mathscr{R}_0^2}, I_1^* = \dfrac{(\psi\eta_2 + \xi\alpha)\beta\omega\mu_h\pi_2\pi_1(\mathscr{R}_0^2 - 1)}{\eta_1\eta_2\eta_3\mu_h(\beta\omega\pi_2 + \eta_5\mu_m\mu_h)\mathscr{R}_0^2} \\ I_2^* = \dfrac{(\eta_3(\rho\eta_2 + \alpha\phi) + \sigma(\psi\eta_2 + \xi\alpha))\beta\omega\mu_h\pi_1\pi_2(\mathscr{R}_0^2 - 1)}{\eta_1\eta_2\eta_3\eta_4\mu_h(\beta\omega\pi_2 + \eta_5\mu_m\mu_h)\mathscr{R}_0^2}, S_2^* = \dfrac{\pi_2}{\Omega + \mu_m} \\ E_2^* = \dfrac{\Omega\pi_2}{\eta_5(\Omega + \mu_m)}, I_3^* = \dfrac{\omega\pi_2\mu_h(\mathscr{R}_0^2 - 1)}{\eta_5\mu_h\mathscr{R}_0^2 + \beta\omega\pi_2} \end{cases}$$

$$\Omega = \frac{[\beta_2\alpha\eta_3\eta_4 + \beta_1(\eta_3(\rho\eta_2 + \alpha\phi) + \sigma(\psi\eta_2 + \xi\alpha)) + \beta_3(\psi\eta_2 + \xi\alpha)]\beta\omega\mu_h\pi_1\pi_2(\mathscr{R}_0^2 - 1)}{\eta_1\eta_2\eta_3\eta_4\mu_h(\beta\omega\pi_2 + \eta_5\mu_m\mu_h)\mathscr{R}_0^2}$$

2.4.1. The Global Stability Analysis of Endemic Equilibrium E^*

Theorem 2. *Model System (2) exhibits a unique endemic equilibrium E^* whenever $\mathscr{R}_0 > 1$, which is globally asymptotically stable.*

Proof 1. We consider vector components $\boldsymbol{Y} = (S_1, E_1, A, I_1, I_2, S_2, E_2, I_3) \in \mathbb{R}_+^8$ and define a Lyapunov function G as follows:

$$G = k_1\left[S_1 - S_1^* - S_1^* \ln\left(\frac{S_1}{S_1^*}\right)\right] + k_2\left[E_1 - E_1^* - E_1^* \ln\left(\frac{E_1}{E_1^*}\right)\right] + k_3\left[A - A^* - A^* \ln\left(\frac{A}{A^*}\right)\right] + k_4\left[I_1 - I_1^* - I_1^* \ln\left(\frac{I_1}{I_1^*}\right)\right] + k_5\left[I_2 - I_2^* - I_2^* \ln\left(\frac{I_2}{I_2^*}\right)\right] + k_6\left[S_2 - S_2^* - S_2^* \ln\left(\frac{S_2}{S_2^*}\right)\right] + k_7\left[E_2 - E_2^* - E_2^* \ln\left(\frac{E_2}{E_2^*}\right)\right] + k_8\left[I_3 - I_3^* - I_3^* \ln\left(\frac{I_3}{I_3^*}\right)\right] \tag{11}$$

By differentiating Equation (11) with respect to t, we have

$$\frac{dG}{dt} = k_1\left(1 - \frac{S_1}{S_1^*}\right)\frac{S_1}{dt} + k_2\left(1 - \frac{E_1}{E_1^*}\right)\frac{E_1}{dt} + k_3\left(1 - \frac{A}{A^*}\right)\frac{A}{dt} + k_4\left(1 - \frac{I_1}{I_1^*}\right)\frac{I_1}{dt} + k_5\left(1 - \frac{I_2}{I_2^*}\right)\frac{I_2}{dt} + k_6\left(1 - \frac{S_2}{S_2^*}\right)\frac{S_2}{dt} + k_7\left(1 - \frac{E_2}{E_2^*}\right)\frac{E_2}{dt} + k_8\left(1 - \frac{I_3}{I_3^*}\right)\frac{I_3}{dt} \tag{12}$$

Let $a = S_1/S_1^*$, $b = E_1/E_1^*$, $c = A/A^*$, $d = I_1/I_1^*$, $p = I_2/I_2^*$, $q = S_2/S_2^*$, $r = E_2/E_2^*$, and $t = \lambda/\lambda^*$.

Substituting equations in Equation (2) into Equation (12) gives the following expression of each term:

$$\begin{cases} k_1\left[-\mu_h S_1\left(1 - \frac{1}{a}\right)^2 + k_1\beta I_3^* S_1^*(1 - as)\left(1 - \frac{1}{a}\right)\right] \\ k_2\beta I_3^* S_1^*\left(1 + as - b - \frac{as}{b}\right) \\ k_3\alpha E_1^*\left(1 + b - c - \frac{b}{d}\right) \\ k_4\left[\psi E_1^*\left(1 + b - d - \frac{b}{d}\right) + \xi A^*\left(1 + c - d - \frac{c}{d}\right)\right] \\ k_5\left[\rho E_1^*\left(1 + b - p - \frac{b}{p}\right) + \phi A^*\left(1 + c - p - \frac{c}{p}\right) + \sigma I_1^*\left(1 + d - p - \frac{d}{p}\right)\right] \\ k_6\left[-\mu_m S_2\left(1 - \frac{1}{q}\right)^2 + \lambda^* S_2^*\left(1 + t - qt - \frac{1}{q}\right)\right] \\ k_7\lambda^* S_2^*\left(1 + qt - r - \frac{qt}{r}\right) \\ k_8\omega E_2^*\left(1 + r - s - \frac{r}{s}\right) \end{cases} \tag{13}$$

Summing up all expressions in Equation (13) and evaluating the values of k_i, $i = 1, 2, \cdots, 8$ gives

$$\begin{cases} k_1 = k_2 = \frac{1}{\beta I_3^* S_1^*}\left[\xi A^* + \psi E_1^* + \frac{\phi\psi A^* E_1^*}{\sigma I_1^*} + \frac{\xi\psi(A^*)^2}{\sigma I_1^*} + \frac{\psi\rho(E_1^*)^2}{\sigma I_1^*} + \frac{\xi\rho A^* E_1^*}{\sigma I_1^*}\right] \\ k_3 = \frac{1}{\alpha E_1^*}\left[\xi A^* + \frac{\phi\psi A^* E_1^*}{\sigma I_1^*} + \frac{\xi\psi(A^*)^2}{\sigma I_1^*}\right], k_4 = 1, k_5 = \frac{\psi E_1^*}{\sigma I_1^*} + \frac{\xi A^*}{\sigma I_1^*} \\ k6 = k_7 = \frac{\beta I_3^* S_1^* k_1}{\lambda^* S_2^*}, k_8 = \frac{\beta I_3^* S_1^* k_1}{\omega E_2^*} \end{cases}$$

Back substitution into Equation (13) and adding up gives

$$\begin{aligned} \frac{dG}{dt} = {} & -k_1\mu_h S_1\left(1 - \frac{1}{a}\right)^2 - k_6\mu_m S_2\left(1 - \frac{1}{q}\right)^2 \\ & + \left(8 - \frac{1}{a} - \frac{as}{b} - \frac{b}{c} - \frac{c}{d} - p - \frac{d}{p} - \frac{1}{q} + t - \frac{qt}{r} - \frac{r}{s}\right)\xi A^* \\ & + \left(7 - \frac{1}{a} - \frac{as}{b} - \frac{b}{d} - p - \frac{d}{p} - \frac{1}{q} + t - \frac{qt}{r} - \frac{r}{s}\right)\psi E_1^* \\ & + \left(7 - \frac{1}{a} - \frac{as}{b} - \frac{b}{c} - p - \frac{c}{p} - \frac{1}{q} + t - \frac{qt}{r} - \frac{r}{s}\right)\frac{\phi\psi A^* E_1^*}{\sigma I_1^*} \\ & + \left(7 - \frac{1}{a} - \frac{as}{b} - \frac{b}{c} - p - \frac{c}{p} - \frac{1}{q} + t - \frac{qt}{r} - \frac{r}{s}\right)\frac{\xi\phi(A^*)^2}{\sigma I_1^*} \\ & + \left(6 - \frac{1}{a} - \frac{as}{b} - p - \frac{b}{p} - \frac{1}{q} + t - \frac{qt}{r} - \frac{r}{s}\right)\frac{\psi\rho(E_1^*)^2}{\sigma I_1^*} \\ & + \left(6 - \frac{1}{a} - \frac{as}{b} - p - \frac{b}{p} - \frac{1}{q} + t - \frac{qt}{r} - \frac{r}{s}\right)\frac{\xi\rho A^* E_1^*}{\sigma I_1^*} \end{aligned} \tag{14}$$

If an algebraic inequality $1 - z \le -\ln z$, for any $z > 0$, then we express all terms in Equation (14) as follows:

Considering the third term, we have:

$$\begin{aligned} & \left[\left(1 - \frac{1}{a}\right) + \left(1 - \frac{1}{q}\right) + (1 - p) + \left(1 - \frac{as}{b}\right) + \left(1 - \frac{b}{c}\right) + \left(1 - \frac{c}{d}\right) + \left(1 - \frac{d}{p}\right) + \left(1 - \frac{qt}{r}\right) + \left(1 - \frac{r}{s}\right) - (1 - t)\right]\xi A^* \le \left[-\ln\left(\frac{1}{a}\right) - \ln\left(\frac{1}{q}\right) - \ln p - \ln\left(\frac{as}{b}\right) - \ln\left(\frac{b}{c}\right) - \ln\left(\frac{c}{d}\right) - \ln\left(\frac{d}{p}\right) - \ln\left(\frac{qt}{r}\right) - \ln\left(\frac{r}{s}\right) + \ln(t)\right]\xi A^* \\ & = [\ln(a) + \ln(q) - \ln(p) - \ln(a) - \ln(s) + \ln(b) - \ln(b) + \ln(c) - \ln(c) + \ln(d) - \ln(d) - \ln(p) - \ln(q) - \ln(t) + \ln(r) - \ln(r) + \ln(s) + \ln(t)]\xi A^* = 0 \end{aligned} \tag{15}$$

A similar approach is applied to all terms. It is evident that $dG/dt \le 0$. Moreover, applying the Krasovkii–Lasalle theorem in Equation (14), $dG/dt = 0$, if and only if $\boldsymbol{Y} = E^*$. Hence, the set consists of the singleton E^*. This concludes the proof. □

2.5. Model Sensitivity Analysis. In this subsection, we utilize Latin hypercube sampling-partial rank correlation coefficient (LHS-PRCC) as a tool for sensitivity and uncertainty. The LHS-PRCC algorithm is robust and particularly suitable for nonlinear systems with a consistent relationship between input and output [17]. The algorithm integrates both uniform and normal probability density functions. This method is recognized for its effectiveness in managing nonlinear ordinary differential equations [22]. Moreover, it quantifies

the level of the linear relationship between inputs and outputs to furnish PRCC indices, following the methodology described by [23]. The variable $I_3(t)$ in Model (2) is used as a showcase to demonstrate the change of PRCC indices with time.

The findings from the LHS-PRCC analysis offered valuable insights into the impact of all parameters against the chosen variable and associated uncertainties on System (2). In the context of statistical inference, PRCC indices close to or equal to zero have no significance. Figure 3(a) visually represents the PRCC indices, highlighting that π_2, β, and β_2 on outputs have strong directly proportion relationship. Conversely, parameters like μ_h and μ_m demonstrating the relationship in inverse proportionally with the model outputs. Figure 3(b) provides a comprehensive view of their sensitivity and illustrates how changes in all parameters influence Model (2). These findings suggest the important variables to be considered for effective control strategies.

2.6. CTMC Stochastic Model Formulation. To assess probabilities of extinction or persistence, the CTMC model was formulated using the technique of events from the process of multitype branching. Capturing the real-world phenomena in the dynamics of lymphatic filariasis, incorporating randomness, is necessary for uncertainties and variabilities [24, 25]. The disease can vanish even when the threshold exceeds one, depending on the initial number of infections available in the population. This study considers individual movement to be discrete for realistic depiction [13, 14].

The formulation of the CTMC stochastic model is derived from System (2) events.

If S_1, E_1, A, I_1, I_2, S_2, E_2, and I_3 represent discrete random variables, then the vector associated is

$$\vec{V} = [S_1, E_1, A, I_1, I_2, S_2, E_2, I_3]^T$$

which follow the Markov chain property and adhere to homogeneity in time. Moreover, the total event is defined by

$$\begin{aligned}\Psi\left(\vec{V}\right) = {} & \pi_1 + \beta I_3 S_1 + \mu_h S_1 + \alpha E_1 + \rho E_1 + \psi E_1 + \mu_h E_1 + \xi A \\ & + \phi A + \mu_h A + \sigma I_1 + \mu_h I_1 + \delta I_2 + \mu_h I_2 + \pi_2 + \beta_2 A S_2 \\ & + \beta_3 I_1 S_2 + \beta_1 I_2 S_2 + \mu_m S_2 + \omega E_2 + \mu_m E_2 + \mu_m I_3\end{aligned} \tag{16}$$

We define $S_1(0) = \pi_1/\mu_h$ and $S_2(0) = \pi_2/\mu_m$, where infectives of type i, denoted as I_i, give rise to infectives of type j, denoted as I_j. It is assumed that the number of offspring produced by an individual of type i is independent of the number of offspring produced by either type i or type j, where $j \neq i$ [14, 26].

This calculation assumes there is initially only one infectious individual at the beginning of the disease outbreak ($I(0) = 1$), with all other types being zero ($I_j = 0$).

$$p_i(u_1, u_2, \cdots, u_n) = \sum_{k_n=0}^{\infty} \cdots \sum_{k_1=0}^{\infty} p_i(k_1, k_2, \cdots, k_6) u_1^{k_1} \cdots u_6^{k_6} \tag{17}$$

where $p_i(k_1, k_2, \cdots, k_n)$ represents the likelihood that an infectious individual of type i produces k_j individuals of type j.

Filariasis extinction is defined by probability $\mathbb{P}_0 = r_1^{i1} r_2^{i2} \cdots r_k^{i6}$, where $(r_1, r_2, \cdots, r_k)$ is the unique fixed point of the offspring pgf, $p_i(r_1, r_2, \cdots, r_6) = r_i$, and $0 < r_i < 1$ for $i = 1, 2, \cdots, k$, whereas $1 - \mathbb{P}_0$ is an outbreak probability.

If $E_1(0) = 1$, $A(0) = 0$, $I_1(0) = 0$, $I_2(0) = 0$, $E_2(0) = 0$, and $I_3(0) = 0$, the offspring probability generating function for the infected class E_1 is defined as follows:

$$p_1(u_1, u_2, \cdots, u_6) = \frac{\alpha u_2 + \psi u_3 + \rho u_4 + \mu_h}{\alpha + \phi + \rho + \mu_h} \tag{18}$$

where $\alpha/(\alpha + \phi + \rho + \mu_h)$ stands for the probability of $E_1(t)$ progress to the $A(t)$, $\psi/(\alpha + \phi + \rho + \mu_h)$ represents the probability of $E_1(t)$ progress to $I_1(t)$, $\rho/(\alpha + \phi + \rho + \mu_h)$ denotes the probability of $E_1(t)$ progress to $I_2(t)$, and $\mu_h/(\alpha + \phi + \rho + \mu_h)$ is the probability of $E_1(t)$ die before any progress

Using a methodology employed in Equation (18), we derive the offspring probability-generating functions for $A(0)$, $I_1(0)$, $I_2(0)$, $E_2(0)$, and $I_3(0)$ as p_2, p_3, p_4, p_5, and p_6, respectively. These functions are defined as follows:

$$\begin{cases} p_2(u_1, u_2, \cdots, u_6) = \dfrac{\xi u_3 + \phi u_4 + \mu_h + \widehat{\beta}_2 u_2 u_5}{\xi + \phi + \mu_h + \widehat{\beta}_2}, \widehat{\beta}_2 = \dfrac{\beta_2 \pi_2}{\mu_m} \\ p_3(u_1, u_2, \cdots, u_6) = \dfrac{\sigma u_4 + \mu_h + \widehat{\beta}_3 u_3 u_5}{\sigma + \mu_h + \widehat{\beta}_3}, \widehat{\beta}_3 = \dfrac{\beta_3 \pi_2}{\mu_m} \\ p_4(u_1, u_2, \cdots, u_6) = \dfrac{\widehat{\beta}_1 u_4 u_5 + \delta + \mu_h}{\widehat{\beta}_1 + \delta + \mu_h}, \widehat{\beta}_1 = \dfrac{\beta_1 \pi_2}{\mu_m} \\ p_5(u_1, u_2, \cdots, u_6) = \dfrac{\omega u_6 + \mu_m}{\omega + \mu_m} \\ p_6(u_1, u_2, \cdots, u_6) = \dfrac{\widehat{\beta} u_1 u_6 + \mu_m}{\widehat{\beta} + \mu_m}, \widehat{\beta} = \dfrac{\beta \pi_1}{\mu_h} \end{cases} \tag{19}$$

The expectation matrix $\mathbb{M} = [m_{ji}]$ computed from the number of offspring of type j resulted from type i as presented by evaluating at 1:

$$\mathbb{M} = \left.\frac{\partial p_i}{\partial u_j}\right|_{u=1} \tag{20}$$

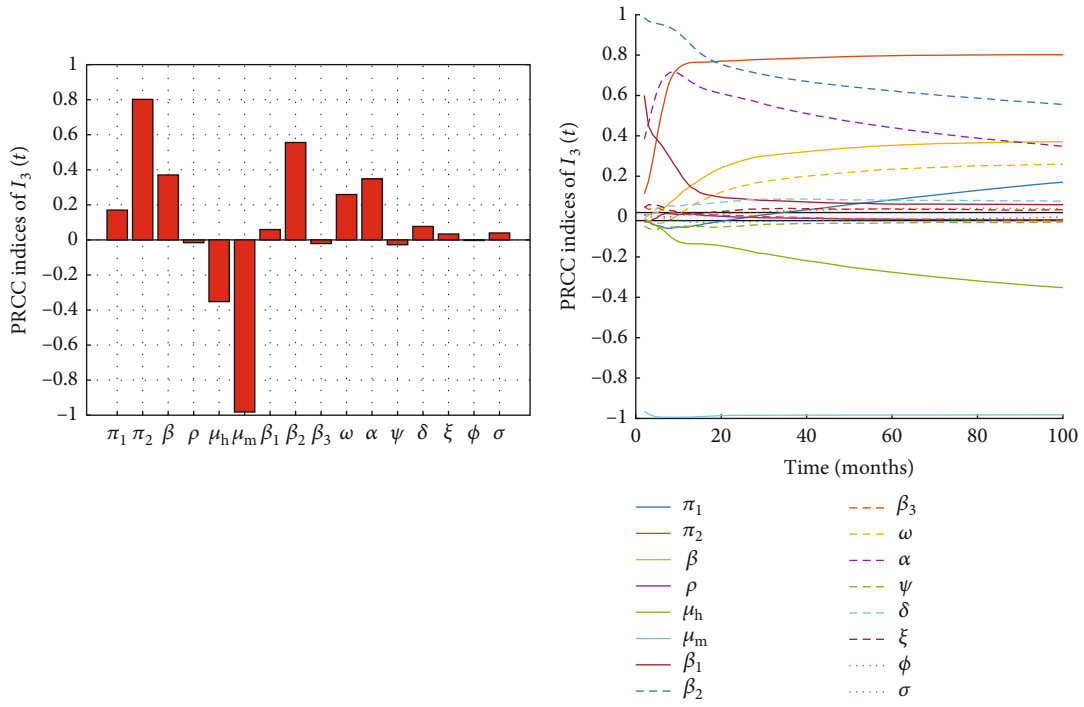

(a) Indices at $t = 100$

(b) The changes of indices

Figure 3: PRCC indices values and dynamics of parameters for $I_3(t)$.

Table 1: Parameter values month^{-1}.

Parameter	Baseline	Reference	Range	Normal (mean (μ), std (σ))
π_1	20.0000	[16]	[10.000030.0000]	$\mathcal{N}(20.0000,2.2048)$
β	0.0005	[17]	[0.000100.0050]	$\mathcal{N}(0.0005,6.2\times10^{-4})$
β_1	0.0015	[17]	[0.00100.0030]	$\mathcal{N}(0.0015,6.6\times10^{-4})$
β_2	0.0035	[17]	[0.00150.0045]	$\mathcal{N}(0.0035,7.9\times10^{-4})$
β_3	0.00025	[17]	[0.000150.00035]	$\mathcal{N}(0.00025,5.0\times10^{-4})$
ρ	0.00032	[17]	[0.000250.0075]	$\mathcal{N}(0.00032,1.0\times10^{-3})$
ψ	0.0015	[30]	[0.00250.0085]	$\mathcal{N}(0.0015,3.3\times10^{-4})$
δ	0.000015	[9]	[0.000010.00003]	$\mathcal{N}(0.000015,3.7\times10^{-4})$
ω	0.0055	[17]	[0.00350.0065]	$\mathcal{N}(0.0055,3.32\times10^{-4}$
ϕ	0.00045	[17]	[0.00030.0009]	$\mathcal{N}(0.00045,5.0\times10^{-4})$
π_2	100,000	[16]	[50000150000]	$\mathcal{N}(100000,598.96)$
μ_h	0.0142	[15, 17]	[0.01000.0200]	$\mathcal{N}(0.0142,1.0\times10^{-4})$
α	0.0200	[9]	[0.01000.0500]	$\mathcal{N}(0.02,5\times10^{-3})$
μ_m	0.050000	[30]	[0.01001.5000]	$\mathcal{N}(0.05000,0.0062)$
ξ	0.00030	[16, 18]	[0.00250.0055]	$\mathcal{N}(0.00030,7.905\times10^{-4})$
σ	0.0012	[10]	[0.00100.0030]	$\mathcal{N}(0.0012,1.87\times10^{-4})$

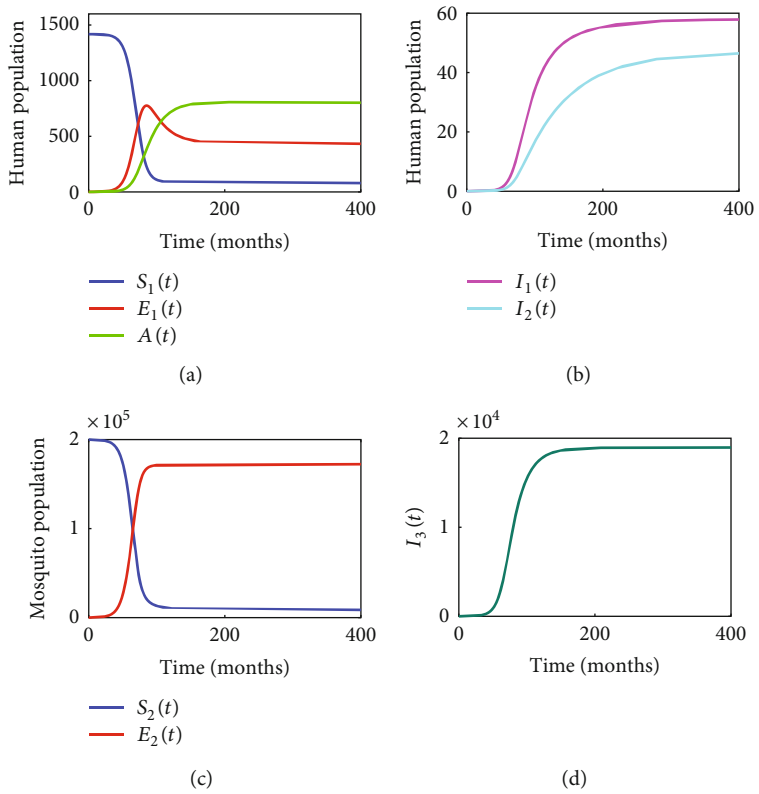

Figure 4: Deterministic dynamics of human and mosquito populations.

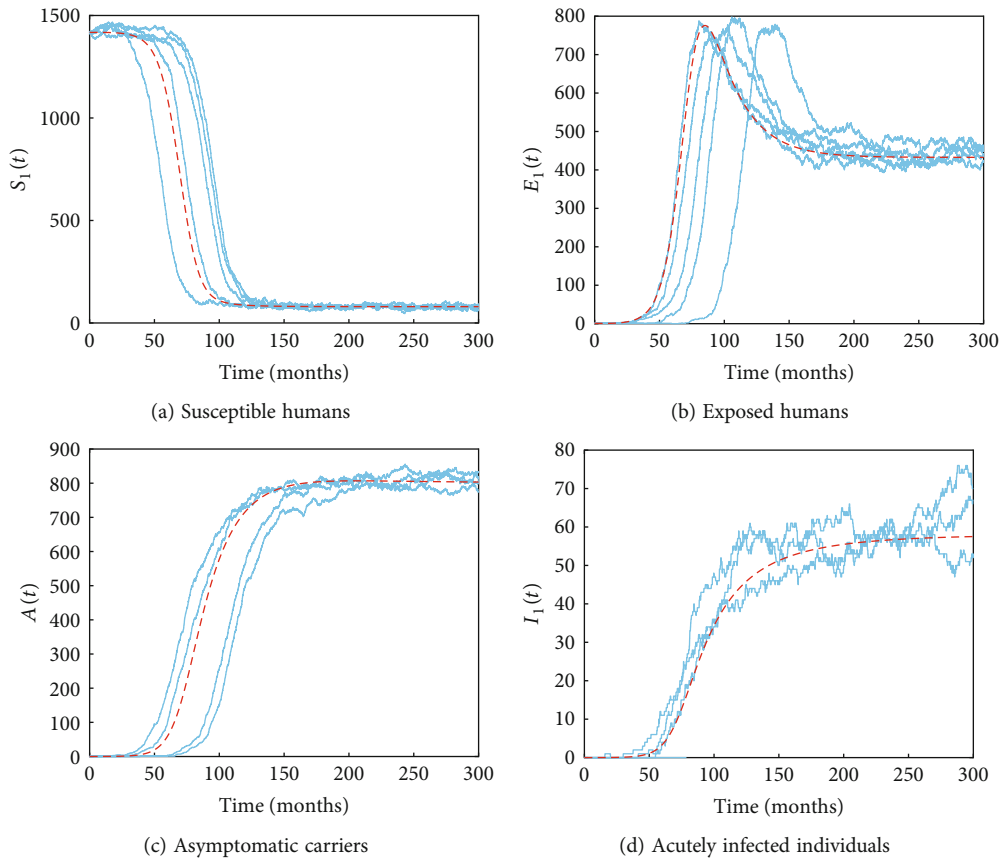

Figure 5: Deterministic (dotted) and CTMC random trajectories for dynamics of lymphatic filariasis in human populations.

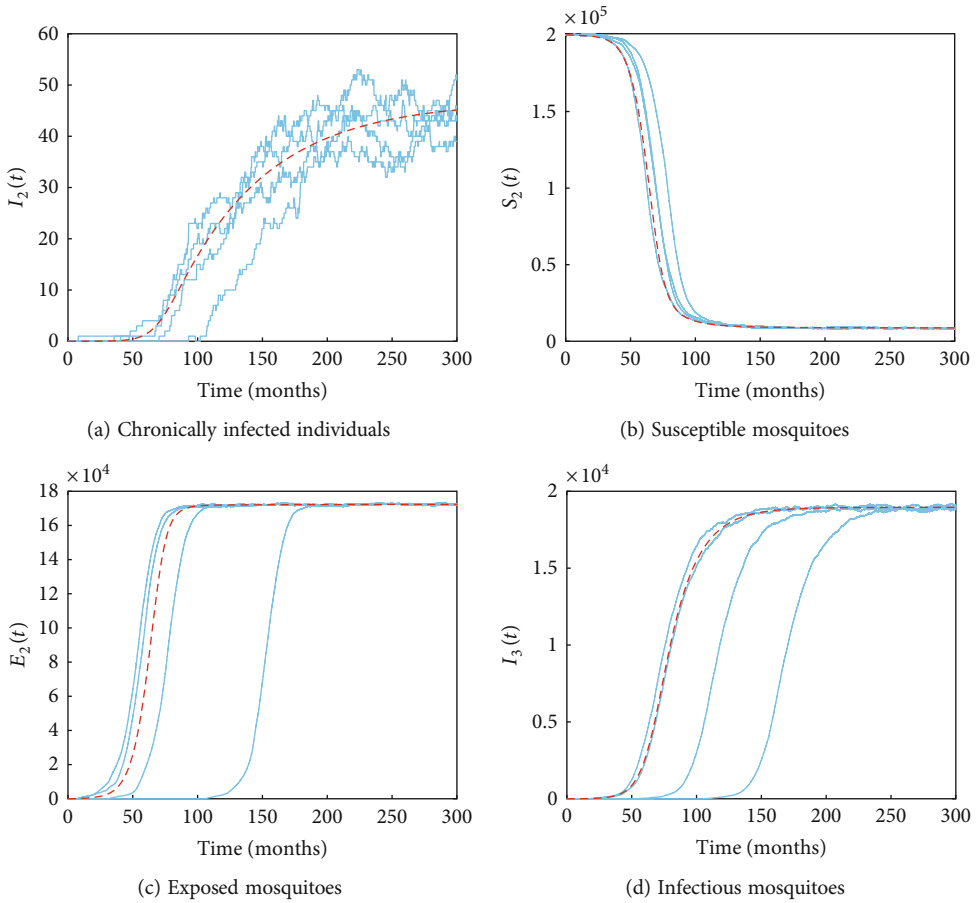

(a) Chronically infected individuals (b) Susceptible mosquitoes

(c) Exposed mosquitoes (d) Infectious mosquitoes

FIGURE 6: Deterministic (dotted) and CTMC random trajectories for dynamics of lymphatic filariasis in (a) human and (b–d) mosquito populations.

Using Equation (20) in conjunction with Equations (18) and (19), we derive

$$\mathbb{M} = \begin{pmatrix} 0 & 0 & 0 & 0 & 0 & \dfrac{\widehat{\beta}}{\left(\widehat{\beta}+\mu_h\right)} \\ \dfrac{\alpha}{G_1} & \dfrac{\widehat{\beta}_2}{G_2} & 0 & 0 & 0 & 0 \\ \dfrac{\psi}{G_1} & \dfrac{\xi}{G_2} & \dfrac{\widehat{\beta}_3}{G_3} & 0 & 0 & 0 \\ \dfrac{\rho}{G_1} & \dfrac{\phi}{G_2} & \dfrac{\sigma}{G_3} & \dfrac{\widehat{\beta}_1}{\left(\widehat{\beta}_1+\mu_h+\delta\right)} & 0 & 0 \\ 0 & \dfrac{\widehat{\beta}_2}{G_2} & \dfrac{\widehat{\beta}_3}{G_3} & \dfrac{\widehat{\beta}_1}{\left(\widehat{\beta}_1+\mu_h+\delta\right)} & 0 & 0 \\ 0 & 0 & 0 & 0 & \dfrac{\omega}{\omega+\mu_m} & \dfrac{\widehat{\beta}}{\left(\widehat{\beta}+\mu_h\right)} \end{pmatrix}$$

where $G_1 = \alpha + \rho + \psi + \mu_h$, $G_2 = \xi + \phi + \mu_h + \widehat{\beta}_2$, and $G_3 = \sigma + \mu_h + \widehat{\beta}_3$. From matrix $\mathbb{M}$, it is straightforward to determine the maximum eigenvalue which represents the stochastic threshold. The correlation between the deterministic and stochastic thresholds for parasite extinction is expressed as $\mathscr{R}_0 < 1 \Leftrightarrow \rho(\mathbb{M}) < 1$ [27, 28]. If $\rho(\mathbb{M}) > 1$, there exists the potential for a microfilarial parasite outbreak or extinction, contingent upon the number of infectives at the onset of the disease outbreak [13, 26, 29]. Therefore, when $\rho(\mathbb{M}) > 1$, a fixed point $(r_1, r_2, r_3, r_4, r_5, r_6) \in (0,1)^6$ is determined from the offspring-generating functions (Equations (18) and (19)), which are utilized to compute the probability of disease extinction [14, 25]. To ascertain this fixed point, the equations $p_i(r_1, r_2, r_3, r_4, r_5, r_6) = r_i$ for $i = 1, 2, \cdots, 6$ are solved.

$$\begin{cases} r_1 = \dfrac{\alpha r_2 + \psi r_3 + \rho r_4 + \mu_h}{\alpha + \psi + \rho + \mu_h}, r_2 = \dfrac{\xi r_3 + \phi r_4 + \mu_h}{\xi + \phi + \mu_h + \widehat{\beta}_2(1 - r_5)}, r_3 = \dfrac{\sigma r_4 + \mu_h}{\sigma + \mu_h + \widehat{\beta}_3(1 - r_5)} \\ r_4 = \dfrac{\delta + \mu_h}{\widehat{\beta}_1(1 - r_5) + \delta + \mu_h}, r_5 = \dfrac{\omega + \widehat{\beta}(1 - r_1) + \mu_m}{(\omega + \mu_m)(\beta(1 - r_1) + \mu_m)}, r_6 = \dfrac{\mu_m}{\widehat{\beta}(1 - r_1) + \mu_m} \end{cases} \tag{21}$$

The probability-generating functions $r_1, r_2, \cdots, r_6$ exhibit nonlinearity, rendering them difficult to compute analytically.

Consequently, numerical simulations, as demonstrated by Stephano et al. [15], are employed for their computation.

3. Model Simulations

In this section, simulations are conducted using both deterministic and CTMC stochastic models to explore the dynamics of lymphatic filariasis. Parameter values, drawn from a Gaussian distribution, are based on baseline values obtained from existing literature, as detailed in Table 1. The simulations involve ten thousand sample trajectories, concurrently depicted with corresponding deterministic solutions to facilitate comparison. Euler's and Gillespie's algorithms are utilized alongside arbitrary initial conditions.

$$\begin{aligned} E_1(0) = 200, A(0) = 20, I_1(0) = 5, I_2(0) = 2, S_1(0) \\ = \frac{\pi_1}{\mu_h} - (E_1(0) + A(0) + I_1(0) + I_2(0)), E_2(0) \\ = 10000, I_3(0) = 1, S_2(0) = \frac{\pi_2}{\mu_m} - (E_2(0) + I_3(0)) \end{aligned}$$

Figure 4, depicting the solutions of the deterministic model, corresponds to Figures 5 and 6, showing both deterministic and CTMC stochastic solutions. It is evident that the count of susceptible individuals decreases following infections, stabilizing after approximately 100 months. Similarly, the population of susceptible mosquitoes diminishes, reaching a steady state. The results reveal that both deterministic and CTMC stochastic models exhibit similar behavior, with stochastic outputs reflecting randomness and deterministic outputs representing the average trend observed across CTMC random sample paths. A negative correlation exists between the susceptible groups and the acutely infected, chronically infected, and asymptomatic classes. Initially, the count of exposed humans rises, peaking within the first 60 months, before declining and eventually stabilizing after 150 months. Similarly, the numbers of asymptomatic, acutely infected, and chronically infected humans also peak before stabilizing.

4. Conclusion

Based on the findings presented in this paper, it is evident that lymphatic filariasis poses a significant threat to human health, causing chronic and irreversible damage to the immune system. Through the development of both deterministic and CTMC stochastic models, this study is aimed at capturing the complexity of lymphatic filariasis dynamics. The deterministic model highlights the potential for disease extinction when the secondary threshold infection number falls below one, contrasting with scenarios where persistence is more likely to occur. Additionally, the role of asymptomatic carriers in disease transmission was identified as significant. These results emphasize the importance of employing stochastic models, such as CTMC, to capture variabilities, randomness, and associated probabilities more accurately, especially considering the limitations of deterministic models in capturing inherent complexities and unpredictabilities.

Data Availability Statement

All data is included in the manuscript.

Conflicts of Interest

The authors declare no conflicts of interest.

Funding

The authors received no specific funding for this work.

References

[1] WHO, "Lymphatic filariasis," World Health Organization, 2022, https://www.who.int/news-room/fact-sheets/detail/lymphatic-filariasis/.

[2] D. Addiss and Eliminate Lymphatic Filariasis, "The 6th meeting of the Global Alliance to Eliminate Lymphatic Filariasis: a half-time review of lymphatic filariasis elimination and its integration with the control of other neglected tropical diseases," vol. 3, no. 1, p. 100, 2010.

[3] S. Lustigman, R. K. Prichard, A. Gazzinelli et al., "A research agenda for helminth diseases of humans: the problem of helminthiases," *PLoS Neglected Tropical Diseases*, vol. 6, no. 4, article e1582, 2012.

[4] CDC, "Parasites - lymphatic filariasis: centers for diseases control and prevention," 2022, https://www.cdc.gov/parasites/lymphaticfilariasis/epi.html.

[5] Centers for Disease Control and Prevention, "Lymphatic filariasis," 2019, January 2023, https://www.cdc.gov/dpdx/lymphaticfilariasis/index.htm.

[6] J. C. Castillo, S. E. Reynolds, and I. Eleftherianos, "Insect immune responses to nematode parasites," *Trends in Parasitology*, vol. 27, no. 12, pp. 537–547, 2011.

[7] P. M. Mwamtobe, S. M. Simelane, S. Abelman, and J. M. Tchuenche, "Mathematical analysis of a lymphatic filariasis model with quarantine and treatment," *BMC Public Health*, vol. 17, no. 1, pp. 1–13, 2017.

[8] P. Jambulingam, S. Subramanian, S. De Vlas, C. Vinubala, and W. Stolk, "Mathematical modelling of lymphatic filariasis elimination programmes in India: required duration of mass drug administration and post-treatment level of infection indicators," *Parasites & Vectors*, vol. 9, no. 1, pp. 501–518, 2016.

[9] E. Michael, M. N. Malecela-Lazaro, P. E. Simonsen et al., "Mathematical modelling and the control of lymphatic filariasis," *The Lancet Infectious Diseases*, vol. 4, no. 4, pp. 223–234, 2004.

[10] S. Swaminathan, P. P. Subash, R. Rengachari, K. Kaliannagounder, and D. K. Pradeep, "Mathematical models for lymphatic filariasis transmission and control: challenges and prospects," *Parasites & Vectors*, vol. 1, no. 1, pp. 1–9, 2008.

[11] E. A. Cromwell, C. A. Schmidt, K. T. Kwong et al., "The global distribution of lymphatic filariasis, 2000–18: a geospatial analysis," *The Lancet Global Health*, vol. 8, no. 9, pp. e1186–e1194, 2020.

[12] L. Allen and A. Burgin, "Comparison of deterministic and stochastic SIS and SIR models," Dept. Math. Technical report, Texas Tech. University, 1999.

[13] M. Maliyoni, "Probability of disease extinction or outbreak in a stochastic epidemic model for West Nile virus dynamics in birds," *Acta Biotheoretica*, vol. 69, no. 2, pp. 91–116, 2021.

[14] M. Maliyoni, F. Chirove, H. D. Gaff, and K. S. Govinder, "A stochastic tick-borne disease model: exploring the probability of pathogen persistence," *Bulletin of Mathematical Biology*, vol. 79, no. 9, pp. 1999–2021, 2017.

[15] M. A. Stephano, J. I. Irunde, J. A. Mwasunda, and C. S. Chacha, "A continuous time Markov chain model for the dynamics of bovine tuberculosis in humans and cattle," *Ricerche di Matematica*, pp. 1–27, 2022.

[16] M. A. Stephano, J. I. Irunde, M. M. Mayengo, and D. Kuznetsov, "The randomness and uncertainty in dynamics of lymphatic filariasis: CTMC stochastic approach," *The European Physical Journal Plus*, vol. 139, no. 2, p. 162, 2024.

[17] M. A. Stephano, M. M. Mayengo, J. I. Irunde, and D. Kuznetsov, "Sensitivity analysis and parameters estimation for the transmission of lymphatic filariasis," *Heliyon*, vol. 9, no. 9, article e20066, 2023.

[18] W. A. Stolk, C. Stone, and S. J. de Vlas, "Modelling lymphatic filariasis transmission and control: modelling frameworks, lessons learned and future directions," *Advances in Parasitology*, vol. 87, pp. 249–291, 2015.

[19] V. Lakshmikantham, S. Leela, and A. A. Martynyuk, *Stability Analysis of Nonlinear Systems*, Springer, 1989.

[20] K. Dietz, "The estimation of the basic reproduction number for infectious diseases," *Statistical Methods in Medical Research*, vol. 2, no. 1, pp. 23–41, 1993.

[21] C. Castillo-Chavez and B. Song, "Dynamical models of tuberculosis and their applications," *Mathematical Biosciences & Engineering*, vol. 1, no. 2, pp. 361–404, 2004.

[22] B. Gomero, "Latin hypercube sampling and partial rank correlation coefficient analysis applied to an optimal control problem, [M.S. thesis]," University of Tennessee, 2012.

[23] S. Marino, I. B. Hogue, C. J. Ray, and D. E. Kirschner, "A methodology for performing global uncertainty and sensitivity analysis in systems biology," *Journal of Theoretical Biology*, vol. 254, no. 1, pp. 178–196, 2008.

[24] L. J. Allen, *An Introduction to Stochastic Processes with Applications to Biology*, CRC press, 2010.

[25] L. J. Allen and G. E. Lahodny Jr., "Extinction thresholds in deterministic and stochastic epidemic models," *Journal of Biological Dynamics*, vol. 6, no. 2, pp. 590–611, 2012.

[26] L. J. Allen and P. van den Driessche, "Relations between deterministic and stochastic thresholds for disease extinction in continuous-and discrete-time infectious disease models," *Mathematical Biosciences*, vol. 243, no. 1, pp. 99–108, 2013.

[27] L. J. Allen, "An introduction to stochastic epidemic models," in *Mathematical Epidemiology*, pp. 81–130, Springer, 2008.

[28] P. Van den Driessche and J. Watmough, "Reproduction numbers and sub-threshold endemic equilibria for compartmental models of disease transmission," *Mathematical Biosciences*, vol. 180, no. 1-2, pp. 29–48, 2002.

[29] G. E. Lahodny and L. J. Allen, "Probability of a disease outbreak in stochastic multipatch epidemic models," *Bulletin of Mathematical Biology*, vol. 75, no. 7, pp. 1157–1180, 2013.

[30] E. Michael, M. N. Malecela-Lazaro, and J. W. Kazura, "Epidemiological modelling for monitoring and evaluation of lymphatic filariasis control," *Advances in Parasitology*, vol. 65, pp. 191–237, 2007.